RM No. L7I30
Copy No.

NACA RM No. L7I30

NACA

RESEARCH MEMORANDUM

15 DEC 1947

YAW CHARACTERISTICS AND SIDEWASH ANGLES OF A 42° SWEPTBACK CIRCULAR-ARC WING WITH A FUSELAGE AND WITH LEADING-EDGE AND SPLIT FLAPS AT A REYNOLDS NUMBER OF 5,300,000

By Reino J. Salmi and James E. Fitzpatrick

Langley Memorial Aeronautical Laboratory
Langley Field, Va.

NATIONAL ADVISORY COMMITTEE
FOR AERONAUTICS

WASHINGTON

December 10, 1947

NATIONAL ADVISORY COMMITTEE FOR AERONAUTICS

RESEARCH MEMORANDUM

YAW CHARACTERISTICS AND SIDEWASH ANGLES OF A 42° SWEPTBACK CIRCULAR-ARC WING WITH A FUSELAGE AND WITH LEADING-EDGE AND SPLIT FLAPS AT A REYNOLDS NUMBER OF 5,300,000

By Reino J. Salmi and James E. Fitzpatrick

SUMMARY

An investigation of the low-speed aerodynamic characteristics in yaw of a 42° sweptback wing of circular-arc airfoil sections was conducted in the Langley 19-foot pressure tunnel. The wing had an aspect ratio of 3.94, taper ratio of 0.625, and neither dihedral nor twist. The tests were made at a Reynolds number of 5,300,000 and a Mach number of 0.11 and included the effects of leading-edge flaps and split flaps and of a fuselage with the wing mounted in high and low positions.

The results of the tests showed that the dihedral effect of the plain wing was maximum at a lift coefficient of 0.35 and was negative for lift coefficients above 0.60. Deflection of the split flaps caused the effective-dihedral parameter to remain fairly constant throughout the lift range at a value of about 0.002, but an almost linear increase with increasing lift occurred when both the leading-edge flaps and split flaps were deflected. In general, the fuselage increased the dihedral when the wing was in the high position and decreased the effective dihedral when the wing was in the low position. With the flaps neutral, however, the fuselage effect was reversed except in the low lift range. A rapid increase in the dihedral effect occurred at maximum lift for all model configurations except for the wing alone when the 0.55-semispan leading-edge flaps and split flaps were deflected.

The plain wing had neutral directional stability with flaps neutral up to a high lift coefficient where it became unstable, but the directional stability increased with increasing lift up to maximum lift for all flap configurations. The fuselage added a destabilizing increment of about 0.001 to the directional-stability parameter for all flap configurations and wing positions.

A comparison of the circular-arc wing with a wing of NACA 64_1-112 sections indicated that, whereas the circular-arc wing showed a rapid decrease in effective dihedral above a lift coefficient of 0.35, the 64-series wing showed a continual increase in effective dihedral up to

maximum lift. With leading-edge flaps there was negligible difference in the variation of effective dihedral with lift coefficient for the two wings.

The results of the air-stream surveys showed that a vertical tail and dorsal fin would be more effective on a low-wing airplane of this type than on a corresponding high-wing airplane.

INTRODUCTION

Supersonic air-flow theory indicates the practicability of using wings with large angles of sweep and sharp-edged airfoil sections for flight at speeds above the speed of sound. In the low-speed range close to maximum lift, the stability of swept-wing aircraft cannot be adequately evaluated from existing theories and, consequently, experimental means of determining their characteristics must be used. Investigations were therefore made in the Langley 19-foot pressure tunnel to determine the aerodynamic characteristics of a 42° sweptback wing of symmetrical circular-arc airfoil sections at a Reynolds number of 5,300,000 and Mach number of 0.11. The longitudinal characteristics of this wing are presented in reference 1. This paper presents the aerodynamic characteristics of the wing in yaw and, also, shows the effects of various wing flaps and of a fuselage on these characteristics with the wing mounted at high and low positions. In order to acquire information concerning the effectiveness of a vertical tail on a swept-wing airplane, air-stream surveys were made to determine the sidewash angles and dynamic-pressure ratios in the region of a vertical tail.

A comparison is shown of the lateral-stability parameters of the circular-arc wing and a wing of nearly identical plan form but employing NACA 64_1-112 airfoil sections.

COEFFICIENTS AND SYMBOLS

The data are referred to a system of axes shown in figure 1. All moments for the wing-fuselage combinations are referred to the assumed center of gravity, which is located on the fuselage center line and in a plane normal to the fuselage center line that passes through the quarter-chord point of the mean aerodynamic chord. The pitching-moment data for the wing alone are referred to the quarter-chord point of the mean aerodynamic chord projected to the plane of symmetry. Standard NACA symbols are used, which are defined as follows:

C_L lift coefficient (Lift/qS)

$C_{L_{max}}$ maximum lift coefficient

C_D drag coefficient (D/qS)

C_X longitudinal-force coefficient (X/qS)

C_Y lateral-force coefficient (Y/qS)

C_l rolling-moment coefficient (L/qSb)

C_m pitching-moment coefficient $(M/qS\bar{c})$

C_n yawing-moment coefficient (N/qSb)

C_{l_ψ} rate of change of rolling-moment coefficient with angle of yaw, per degree $(\partial C_l/\partial \psi)$

C_{n_ψ} rate of change of yawing-moment coefficient with angle of yaw, per degree $(\partial C_n/\partial \psi)$

C_{Y_ψ} rate of change of lateral-force coefficient with angle of yaw, per degree $(\partial C_Y/\partial \psi)$

Lift = -Z

D drag, -X at zero yaw

X longitudinal force

Y lateral force

Z vertical force

L rolling moment

M pitching moment

N yawing moment

α angle of attack of chord line measured in plane of symmetry

ψ angle of yaw, positive when right wing is back

σ sidewash angle, angle between direction of air flow and tunnel center line measured in XY-plane, positive when angle of attack at vertical tail is decreased

σ_{av} average sidewash angle $\left(\int_{0.2}^{1.2} \sigma \, dh\right)$

S wing area

S_t tail area

$\bar{c}$ Mean aerodynamic chord (M.A.C.), measured parallel to plane of symmetry $\left(\frac{2}{S}\int_0^{b/2} c^2\,dy\right)$

c local chord parallel to plane of symmetry

b wing span

y spanwise coordinate

q free-stream dynamic pressure $\left(\frac{1}{2}\rho V^2\right)$

q_t dynamic pressure at tail

V free-stream velocity

ρ mass density of air

R Reynolds number $(\rho V\bar{c}/\mu)$

μ coefficient of viscosity of air

M Mach number (V/a)

a velocity of sound

h height above fuselage center line, fraction of M.A.C.

l longitudinal distance from center of gravity to center of pressure of vertical tail

$\left(\frac{dC_n}{d\psi}\right)_t$ rate of change of yawing-moment coefficient with angle of yaw, due to vertical tail

$\left(\frac{dC_L}{d\alpha}\right)_t$ lift-curve slope of vertical tail

APPARATUS AND TESTS

Model

Figure 2 shows the details of the model. The wing has a sweepback angle of 42.05° along a line joining the leading edges of the root chord and the theoretical tip chord. The aspect ratio is 3.94 and the taper ratio, 0.625. There is no geometric dihedral nor twist. The airfoil sections normal to the line of maximum thickness are symmetrical circular-arc sections having a maximum thickness of 10 percent at the root and 6.4 percent at the tip. A constant radius of 83.26 inches was maintained

for all sections, measured in planes normal to the line of maximum thickness. The leading and trailing edges are therefore parts of an ellipse, with the maximum deviation being 0.4 inch from a straight line joining the leading edges of the root and tip chords. The wing thickness measured in planes parallel to the plane of symmetry is 7.9 percent at the root and 5.2 percent at the tip. The wing was machined from solid steel and was lacquered and sanded to an aerodynamically smooth surface.

The fuselage has a circular cross section tapering to a point at each end and has a fineness ratio of 10.2. The maximum diameter, which is constant at the wing intersection, is equal to 40 percent of the wing chord (measured at the plane of symmetry). The center portion of the fuselage has removable blocks to permit the mounting of the wing at various heights from the fuselage center line. The fuselage was made from laminated mahogany and was lacquered and sanded smooth.

The leading-edge flaps were fabricated from sheet steel on which $\frac{1}{2}$-inch-diameter steel tubing was welded to form a round leading edge. (See figs. 3 and 4.) The flaps had a constant chord of 3.80 inches normal to the leading edge of the wing and were deflected down 37°, measured in a plane normal to the leading edge of the wing. Two flap spans were used, extending from 27.9 percent semispan and 42.5 percent semispan to 97.5 percent semispan.

The trailing-edge split flaps were made from sheet aluminum and extended over the inboard 50 percent of the wing. The inboard 12.5 percent of the split flaps were removable to permit flap deflection with the wing mounted on the fuselage in the high wing position. The split flaps were deflected 60° from the wing lower surface as measured in a plane normal to the flap hinge line. The flap chord was 20 percent of the local wing chord.

A streamlined fairing was used to cover the support-strut fittings near the trailing edge of the wing center section, and a small fairing (fig. 2) was required for the wing-fuselage combinations. A photograph of the model mounted in the tunnel is presented in figure 4.

Tests

Six-component force tests were made in the Langley 19-foot pressure tunnel with the model mounted on a single support (fig. 4) which permitted changes in both the angle of attack and the angle of yaw. The test Reynolds number was 5,300,000, and the corresponding Mach number was 0.11.

Tests of the wing-alone and the wing-fuselage combinations were made with the flaps neutral and with the two leading-edge flaps in conjunction with deflected split flaps. Wing-alone tests were also made with only the split flaps deflected.

The static-stability derivatives were obtained from tests through the angle-of-attack range at 0° and ±5° angle of yaw, and the characteristics in yaw were found from tests made at constant angles of attack with the angle of yaw varying from -5° to 20°.

The air-stream surveys were made with the 19-foot-pressure-tunnel rake (figs. 5(a) and 5(b)) at the locations shown in figure 5(c). The survey plane was always perpendicular to the tunnel center line regardless of the model angle of attack. Sidewash angles and dynamic-pressure ratios at the tail were measured at two angles of attack for the wing alone with flaps neutral and with the $0.55\frac{b}{2}$ leading-edge flaps in conjunction with split flaps, deflected. Surveys were made at three angles of attack for the wing-fuselage combinations with the $0.55\frac{b}{2}$ leading-edge flaps and split flaps deflected and at two angles of attack with the flaps neutral.

Corrections to Data

The lift, drag, and pitching-moment data presented herein have been corrected for support tare and interference effects and for air-stream misalinement. The jet-boundary corrections to the angle of attack and drag coefficient were calculated from reference 2 and are as follows:

$$\Delta\alpha = 1.00C_L$$

$$\Delta C_D = 0.0152C_L^2$$

The correction to the pitching-moment coefficient due to tunnel-induced distortions of the wing loading is

$$\Delta C_m = 0.004C_L$$

No jet-boundary corrections were applied to the rolling-moment, yawing-moment, and lateral-force coefficients.

All corrections were added to the data.

RESULTS AND DISCUSSION

The angle of attack, drag coefficient, and pitching-moment coefficient are plotted against lift coefficient for the plain wing with all flap configurations and are presented in figure 6. The stability parameters C_{l_ψ}, C_{n_ψ}, and C_{Y_ψ} are given as functions of lift coefficient in figures 7 and 8. The results of the extended angle-of-yaw

tests are presented in figures 9 and 10. Figures 11 and 12 show the results of air-stream surveys in the region of the vertical tail.

At the maximum lift coefficient for the plain wing with 0.70 $\frac{b}{2}$ leading-edge flaps, the break in the pitching-moment curve (fig. 6(a)) is opposite to that obtained in reference 1. The stall progression obtained with the 0.70 $\frac{b}{2}$ flaps (reference 1) would not greatly affect the pitching moment unless some external disturbance caused the root or tip stall to be more severe. This change in the pitching-moment characteristics may be caused either by some difference in test setups or by the degree of smoothness of the wing-flap juncture. The 0.55 $\frac{b}{2}$ flap tests do not exhibit this change in the pitching-moment characteristics.

Lateral-Stability Parameters of Plain Wing

Dihedral effect.- The effective-dihedral parameter C_{l_ψ} of the plain wing increased with increasing lift coefficient (fig. 7(a)) to a value of $C_{l_\psi} = 0.00095$ at a C_L of 0.35 and then decreased to zero at a C_L of 0.60, beyond which it decreased to a minimum value of -0.00210 at a C_L of 0.84. The decrease in C_{l_ψ} may be associated with the early tip stalling (reference 1) which, as indicated by stall studies of a similar wing in the Langley full-scale tunnel, starts on the leading wing. Near the maximum lift coefficient, a rapid increase in C_{l_ψ} occurred. These same stall studies showed that the trailing wing remained relatively stall free to a very high angle of attack and a similar tendency on the wing of the present discussion would cause a rapid increase in C_{l_ψ} when the trailing wing finally stalled.

Directional stability and lateral force.- The plain wing had neutral directional stability throughout the lift range except for lift coefficients above 0.73 where the positive values of C_{n_ψ} showed the wing to be slightly unstable. The lateral-force parameter C_{Y_ψ} of the plain wing increases slightly with lift and has a maximum value of 0.0018.

Effect of Wing Flaps on Lateral-Stability Parameters

Dihedral effect.- Figure 7(a) shows that with only the split flaps deflected the values of C_{l_ψ} remained fairly constant at a value of about 0.0020 in the range of moderate lifts but decreased in the high

lift range. When the leading-edge flaps were used in conjunction with the split flaps, C_{l_Ψ} increased with lift coefficient to values of C_{l_Ψ} of 0.0059 for the 0.70 $\frac{b}{2}$ leading-edge flaps. This variation in C_{l_Ψ} with C_L can be explained by the tuft studies of reference 1, which show that the leading-edge flaps delayed the tip stall to high angles of attack.

Directional stability and lateral force.- For all flap configurations the wing was directionally stable throughout the lift range and C_{n_Ψ} was approximately equal for all flap configurations at corresponding lift coefficients. A decrease in stability occurred near the maximum lift, however, particularly with the 0.70 $\frac{b}{2}$ leading-edge flaps, although positive values of C_{n_Ψ} did not occur at the highest angle of attack tested.

The lateral-force parameter C_{Y_Ψ} remained at a fairly constant value of about 0.001 through the lift range up to $C_{L_{max}}$.

Effects of a Fuselage on Lateral-Stability Parameters

Dihedral effect.- The effects of a circular fuselage on the variation of the effective-dihedral parameter C_{l_Ψ} with lift coefficient are shown in figure 8. In the flaps neutral condition, the high-wing combination showed greater effective dihedral than the wing alone for values of C_L below 0.35, but at values of C_L greater than 0.35, the values of C_{l_Ψ} for the high-wing combination were less positive than those for the wing alone. The effective dihedral of the low-wing combination was negative at lift coefficients below 0.18 but had an almost constant low positive value in the range of C_L from 0.18 to 0.76. This variation of C_{l_Ψ} with C_L contrasts with that of the high-wing combination and the wing alone which showed a rapid decrease in C_{l_Ψ} with increasing C_L. The effects of the fuselage were similar to those observed for low-wing models of reference 4.

When the 0.55 $\frac{b}{2}$ leading-edge flaps and 0.50 $\frac{b}{2}$ split flaps were deflected, the high-wing combination had more positive values of C_{l_Ψ} than the plain wing except for lift coefficients above 1.15. No data were obtained for the high-wing combination with the 0.70 $\frac{b}{2}$ leading-edge

flaps. The low-wing combination had lower effective dihedral throughout the lift range than the plain wing for both leading-edge flap spans.

A reduction in C_{l_ψ} near $C_{L_{max}}$ and then a subsequent rapid increase was evident for all combinations regardless of flap deflection.

Directional stability and lateral force.- The wing-fuselage combinations had values of C_{n_ψ} of about 0.001 more positive than the wing alone, for all flap conditions. The lateral-force parameter C_{Y_ψ} of the wing-fuselage combinations is more positive than that for the wing alone. The low-wing combination had irregular variations of C_{Y_ψ} in the high lift range when the leading-edge flaps were deflected.

Comparison with NACA 64_1-112 Wing

Dihedral effect.- A comparison of the lateral-stability derivatives of the wings with circular-arc sections and NACA 64_1-112 sections (reference 4) is given in figure 7(b). At a Reynolds number of 5,300,000 and with the flaps neutral, the NACA 64_1-112 wing had an almost linear increase in dihedral effect with increasing lift coefficient up to $C_{L_{max}}$. The dihedral effect of the circular-arc wing, however, reached only a small positive value at a C_L of 0.35 and then decreased rapidly. At a Reynolds number of 1,720,000, the variation of C_{l_ψ} with C_L with flaps neutral for the NACA 64_1-112 wing was somewhat similar to that of the circular-arc wing. There was a negligible difference in the variation of C_{l_ψ} with C_L for the two wings at a Reynolds number of 5,300,000 when the leading-edge flaps and split flaps were deflected.

Directional stability and lateral force.- With flaps deflected, the directional stability of the two wings was about equal at a Reynolds number of 5,300,000. With flaps neutral, however, the NACA 64_1-112 wing was directionally stable whereas the circular-arc wing had neutral directional stability. At the lower Reynolds number, however, the 64-series wing was also neutrally stable up to moderate lift coefficients. The circular-arc wing had somewhat more positive values of C_{Y_ψ} than the NACA 64_1-112 wing. The destabilizing effect of the fuselage was similar for both wings.

Characteristics in Extended Yaw Range

Tests through a yaw range of -5° to 20° angle of yaw, showed that the greatest effect due to yaw occurred on the yawing moment of the low-wing combination (fig. 10) at an angle of attack of 17.4°. With the leading-edge flaps and split flaps deflected, a change from a stable (negative) slope to an unstable slope occurred at angles of yaw of 5° for the 0.55 $\frac{b}{2}$ flaps and $\psi = 8^\circ$ for 0.70 $\frac{b}{2}$ flaps. The plain wing (fig. 9) had a change in the variation of rolling moment with angle of yaw at a yaw angle of 10° for $\alpha = 14.8^\circ$. when the curve changed from an unstable (negative) slope to a positive slope.

Air-Flow Characteristics in the Region of a Vertical Tail

Figure 7 and reference 4 show that, in general, an isolated sweptback wing is directionally stable below the stall. A comparison of figure 9 with figure 10, however, shows that the directional instability of the fuselage is great enough to make the combination unstable. A vertical tail is therefore necessary for directional stability on a configuration of this type. Information concerning the effectiveness of a vertical tail may be obtained from the sidewash angles and dynamic-pressure ratios. The dynamic-pressure ratios presented in figures 11 and 12 show values somewhat greater than unity in the region above the wake.

Although dynamic-pressure ratios greater than unity have been observed in the field of flow behind wing-fuselage combinations, the values obtained in this investigation appear somewhat greater than would be expected.

The sidewash angles and dynamic-pressure ratios are related to vertical-tail effectiveness by the following expression:

$$\left(\frac{\partial C_n}{\partial \psi}\right)_t = \left(\frac{dC_L}{d\alpha}\right)_t \left(1 - \frac{\partial \sigma}{\partial \psi}\right) \frac{q_t}{q} \frac{S_t}{S} \frac{l}{b}$$

Although an exact value of $\left(\frac{dC_L}{d\alpha}\right)_t$ cannot be known without actual vertical-tail tests because of tail-fuselage interference, the preceding expression will give fairly accurate values if $\frac{dC_L}{d\alpha}$ of the isolated tail is used.

Under certain of the present test conditions, the flow angularity was in excess of that for which the rake had been calibrated and an

extrapolation was necessary. A straight-line extrapolation was used and the values of the extrapolated sidewash angles are thought to be accurate within $\pm 0.5^\circ$. The extrapolated values are designated on figures 11 and 12 by dot-dash curves. These data have been corrected for the slight variations which may have occurred at zero yaw.

To facilitate the present discussion, the values of sidewash angles presented in figures 11 and 12 have been averaged and the average values are given in table I. These sidewash angles have been corrected for the sidewash angles at zero yaw.

Effect of wing vortex field.- Figure 12(a) represents sidewash angles measured behind the wing alone. Even at the low angle of attack (5.9°), the average sidewash at 15° yaw is as much as -1.3°. At the higher angle of attack and at a value of h of 0.7, the sidewash angles were -2° and -5° at $\psi = 10^\circ$ and 15°, respectively. As there was no fuselage, but only the wing with flaps, the flow angularity appears to be caused by the vortex field of the wing as the wing was yawed; that is, the vortices from the leading wing influenced the side flow while those from the trailing wing were carried downstream. A previous side-flow investigation (reference 5) pointed out that the vortices associated with the span load distribution of the wing of conventional sections and low sweep made a practically negligible contribution to the sidewash angle. However, the present investigation included tests of a wing of lower aspect ratio and of circular-arc sections at higher lifts. The wing vortices were thus stronger and closer to the survey plane.

At the high angles of attack, the lower survey points were found to be in the wake of the wing (fig. 12(a)) inasmuch as $\frac{q_t}{q}$ suddenly decreased.

Effects of fuselage position.- The effect of wing-fuselage interference on the side flow at a vertical tail has been described in reference 3 and is demonstrated by the air-stream surveys of reference 5. In reference 5, fuselage was considered to be a low-aspect-ratio aerodynamic surface with vortices shed from the upper and lower surfaces when the fuselage was yawed. These vortices produce a negative sidewash angle in the region of a vertical tail when the fuselage is at positive yaw. With the wing in the low position, however, the vortices shed from the upper surface of the fuselage were stronger in that the wing acted as an end plate, and they were thus the principal factor in causing an angularity in the flow. Consequently, the effect of interference on the low-wing combination is to cause a greater negative sidewash than that due to the fuselage alone, and this fact is substantiated by the results of reference 5. With the wing in the high position the vortices from the upper surface are weakened; hence the sidewash is less negative than for the fuselage alone.

The results of the present investigation seem to verify the preceding analysis. Figures 12(a) and 12(b) show a close similarity of the sidewash angles for the wing alone and for the high-wing combination. The interference thus appears to cancel the fuselage effect, and the sidewash behind the high-wing combination is due almost entirely to the wing-vortex field described in the preceding section.

On the other hand, the large negative sidewash angles of the low-wing combination (figs. 11(b) and 12(c)) indicate that the combined effects of the fuselage vortices and wing-fuselage interference are large. The greater negative sidewash angles behind the low-wing combination would increase vertical-tail effectiveness but would cause vertical-tail stall at lower angles of yaw. The average values of $\frac{\partial \sigma}{\partial \psi}$ obtained were from -0.2 to -0.3 in the low-wing configuration and from 0 to -0.1 in the high-wing combination.

The increase of negative sidewash near the fuselage in the low-wing configuration (fig. 12(c)) would increase the effectiveness of a dorsal fin in this configuration over that in the high-wing configuration.

Figures 12(b) and 11(a) indicate a sudden diminution in dynamic pressure at the high angles of attack in the high-wing configuration. From the geometry of the model attitude, the lower survey points are seen to be in the wake of the wing, which has stalled near the root as has been previously pointed out. In the low-wing combination, however, (figs. 11(b) and 12(c)) the survey points are mostly above the wing wake and, consequently, the dynamic pressure remains nearer the free-stream value.

Effect of flap deflection.- The influence of flap deflection on the sidewash angles may be seen by referring to table I. A comparison of average sidewash angles at approximately equal angles of attack with flaps deflected and flaps neutral in either the high-wing or low-wing configuration indicates that flaps cause a small decrement. This decrease in sidewash increases with angle of yaw and with angle of attack to a maximum of 1.5° at $\psi = 15^\circ$ and $\alpha = 17.4^\circ$. The decrement in sidewash is probably caused by changes in the span loading of the wing due to flap deflection.

SUMMARY OF RESULTS

The results of an investigation of the aerodynamic characteristics in yaw of a 42° sweptback wing of circular-arc sections and of air-stream surveys in the region of a vertical tail may be summarized as follows:

1. The dihedral effect of the plain wing was maximum at a lift coefficient of 0.35 and was negative for lift coefficients above 0.60.

2. Deflection of the split flaps caused the effective-dihedral parameter to remain fairly constant through the lift range at a value of about 0.002, but an almost linear increase with increasing lift occurred when both the leading-edge flaps and split flaps were deflected.

3. In general, the fuselage increased the dihedral when the wing was in the high position with flaps deflected and decreased the effective dihedral when the wing was in the low position. With the flaps neutral, however, this effect was reversed except in the low lift range.

4. A rapid increase in the dihedral effect occurred at maximum lift for all model configurations except for the wing alone when the 0.55-semispan leading-edge flaps and split flaps were deflected.

5. With flaps neutral the wing alone had neutral directional stability up to a high lift coefficient where it became unstable, but for all flap configurations the wing had increasing directional stability with increasing lift up to maximum lift.

6. The fuselage added a destabilizing increment of about 0.001 to the directional-stability parameter for all flap configurations and wing positions.

7. Comparison of the characteristics of the circular-arc wing with those of a wing of NACA 64_1-112 sections showed that the circular-arc wing had a rapid decrease in effective dihedral with lift coefficient above a lift coefficient of 0.35; whereas for the NACA 64_1-112 wing, the effective dihedral increased continuously up to the maximum lift. With leading-edge flaps, there was negligible difference in the variation of effective dihedral with lift coefficient for the two wings.

8. The results of the air-stream surveys showed that a vertical tail and dorsal fin would be more effective on a low-wing airplane of this type than on a corresponding high-wing airplane.

Langley Memorial Aeronautical Laboratory
National Advisory Committee for Aeronautics
Langley Field, Va.

REFERENCES

1. Neely, Robert H., and Koven, William: Low-Speed Characteristics in Pitch of a 42° Sweptback Wing with Aspect Ratio 3.9 and Circular-Arc Airfoil Sections. NACA RM No. L7H23, 1947.

2. Eisenstadt, Bertram J.: Boundary-Induced Upwash for Yawed and Swept-Back Wings in Closed Circular Wind Tunnels. NACA TN No. 1265, 1947.

3. House, Rufus O., and Wallace, Arthur R.: Wind-Tunnel Investigation of Effect of Interference on Lateral-Stability Characteristics of Four NACA 23012 Wings, an Elliptical and a Circular Fuselage, and Vertical Fins. NACA Rep. No. 705, 1941.

4. Salmi, Reino J., Conner, D. William, and Graham, Robert R.: Effects of a Fuselage on the Aerodynamic Characteristics of a 42° Sweptback Wing at Reynolds Numbers to 8,000,000. NACA RM No. L7E13, 1947.

5. Recant, Isidore G., and Wallace, Arthur R.: Wind-Tunnel Investigation of the Effect of Vertical Position of the Wing on the Side Flow in the Region of the Vertical Tail. NACA TN No. 804, 1941.

TABLE I

AVERAGE SIDEWASH ANGLES

Configuration	α (deg)	ψ (deg)	σ_{av} (deg)
Wing alone, flaps on	5.9	5	-0.3
		10	-.9
		15	-1.3
	15.3	5	.3
		10	.4
		15	.2
Low wing, flaps on	3.6	5	-1.5
		10	-2.6
		15	-4.4
	11.1	5	-2.2
		10	-3.1
		15	-4.5
	17.4	5	-1.4
		10	-3.4
		15	-6.4
High wing, flaps on	3.6	5	-.4
		10	-.9
		15	-1.2
	11.1	5	-.2
		10	-.8
		15	-2.2
	17.4	5	-.3
		10	-1.2
		15	-2.0
Low wing, flaps off	5.4	5	-.9
		10	-2.3
		15	-3.1
	14.9	5	-1.3
		10	-2.9
		15	-4.3
High wing, flaps off	5.4	5	-.2
		10	-.7
		15	-1.2
	14.9	5	.1
		10	-.1
		15	-.4

NATIONAL ADVISORY
COMMITTEE FOR AERONAUTICS

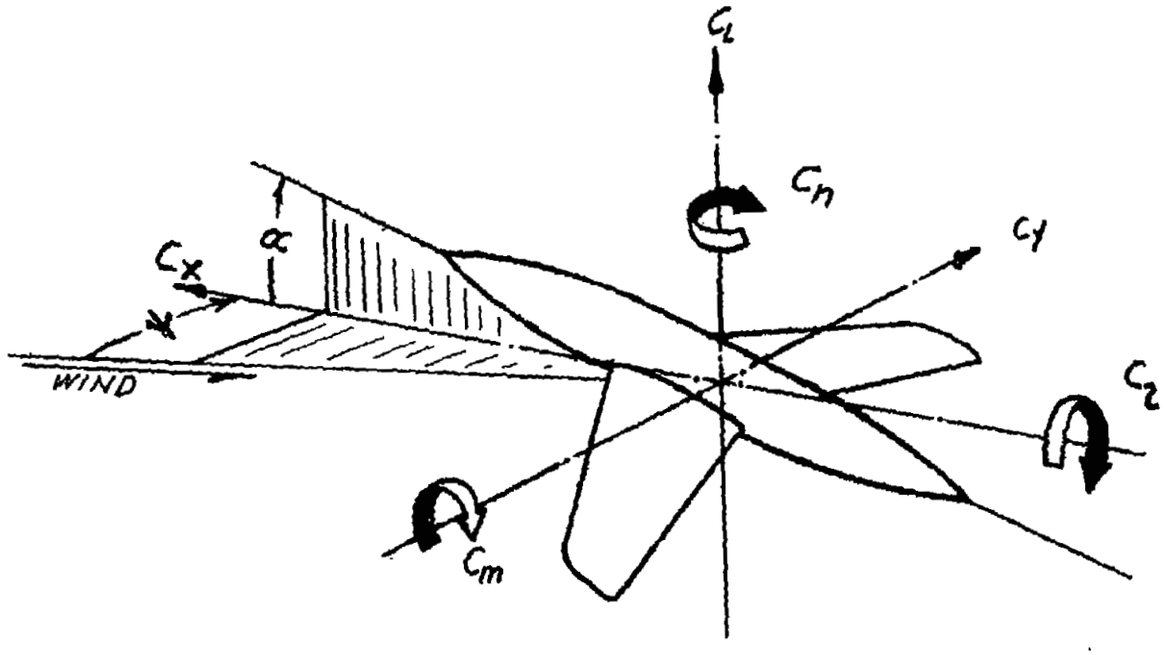

NATIONAL ADVISORY
COMMITTEE FOR AERONAUTICS

Figure 1. - System of axes used. Arrows indicate positive directions.

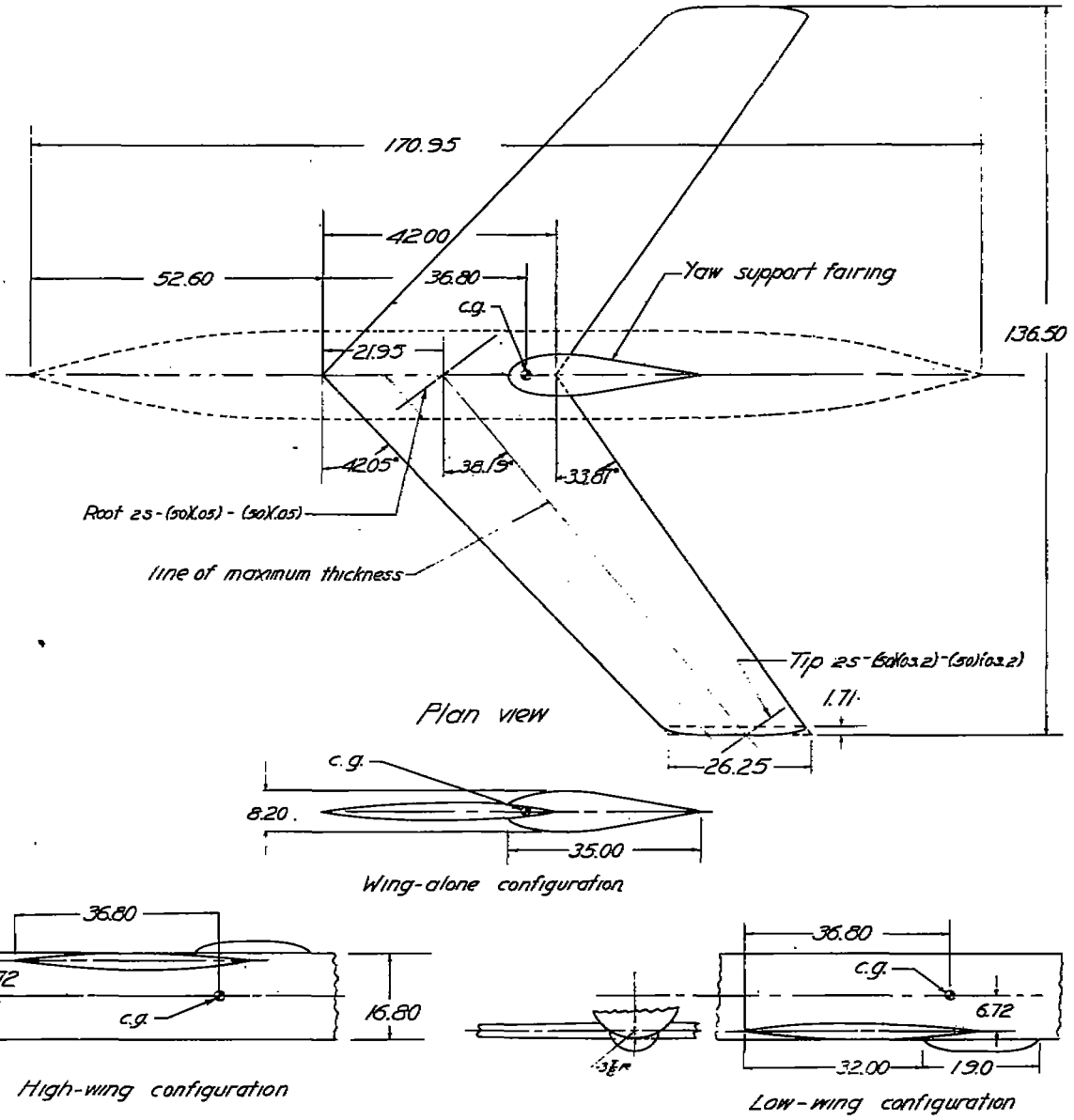

Sections through plane of symmetry

Note: All dimensions in inches

NATIONAL ADVISORY COMMITTEE FOR AERONAUTICS

FUSELAGE ORDINATES			
Distance from nose	Diameter	Distance from nose	Diameter
0	0.2	112.00	16.80
18.00	9.84	122.00	16.32
22.05	11.80	132.00	14.90
27.39	13.80	142.00	12.52
34.56	15.60	151.20	9.46
42.35	16.60	162.00	4.78
48.00	16.80	170.95	0.

Figure 2.- Plan view and details of 42° sweptback wing and fuselage. Wing area = 4728 sq in.; $\bar{c}$ = 35.31 in.; aspect ratio = 3.94. No dihedral or twist.

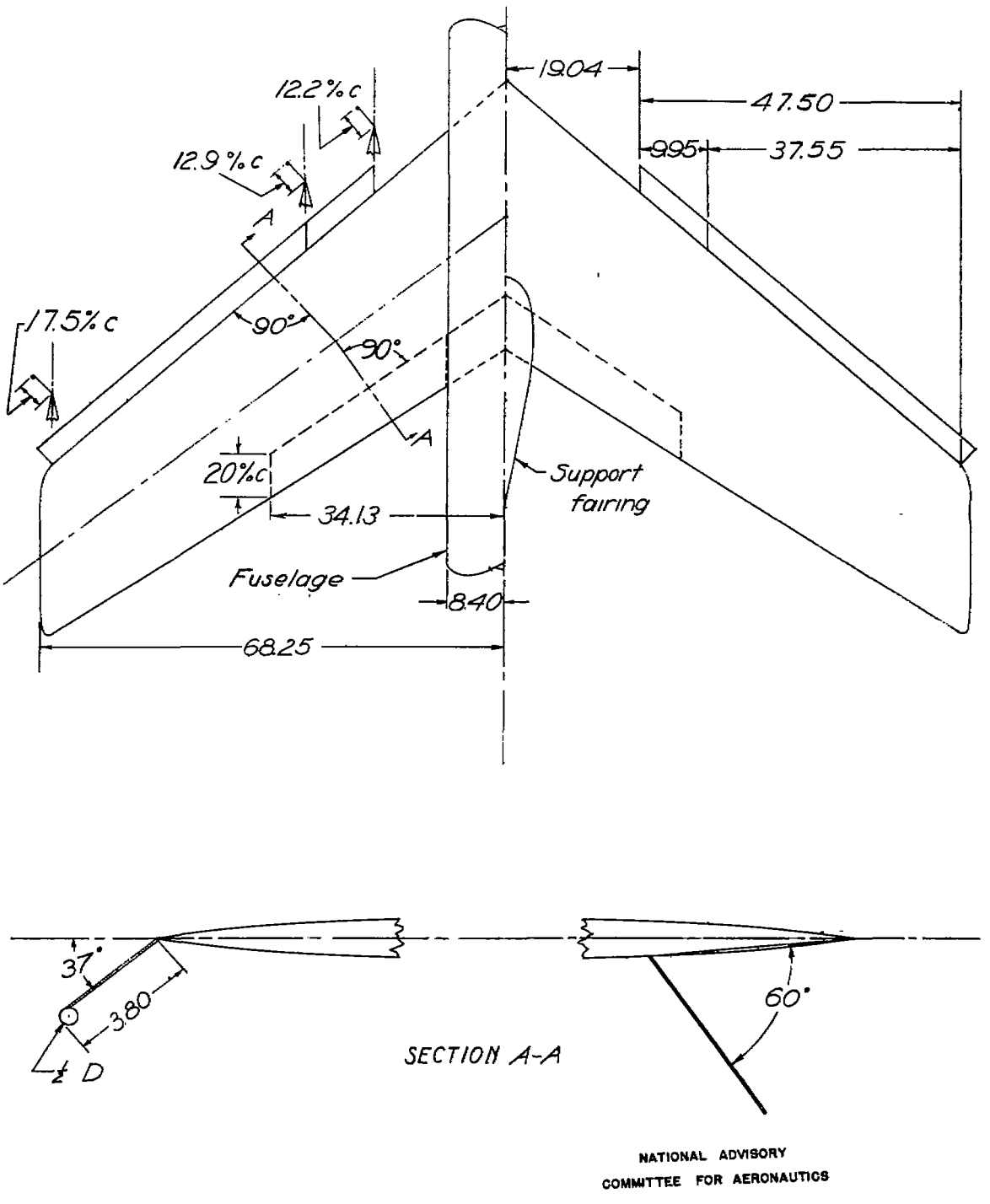

Figure 3.- Geometry of flaps for 42° sweptback wing of circular-arc sections. All dimensions in inches.

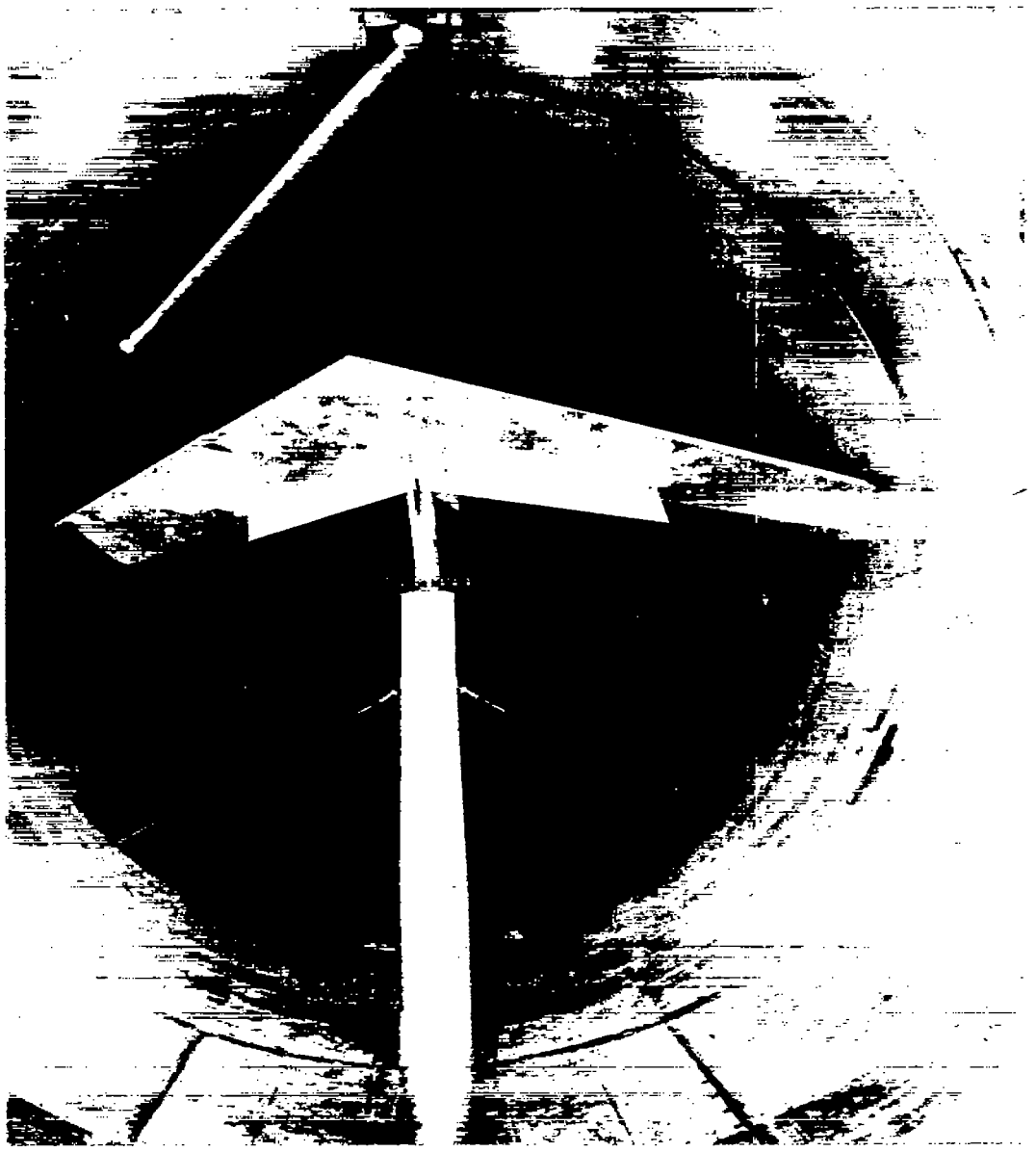

(a) Model installation.

Figure 4.- The 42° sweptback wing of symmetrical circular-arc sections mounted in the Langley 19-foot pressure tunnel.

(b) Details of leading-edge flap.

Figure 4.- Continued.

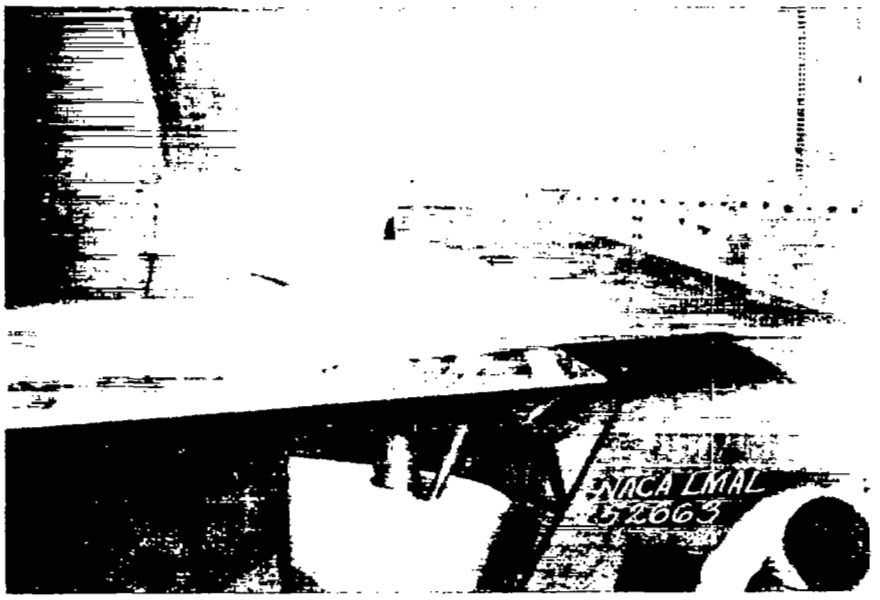

(c) Support-fairing details.

Figure 4.- Concluded.

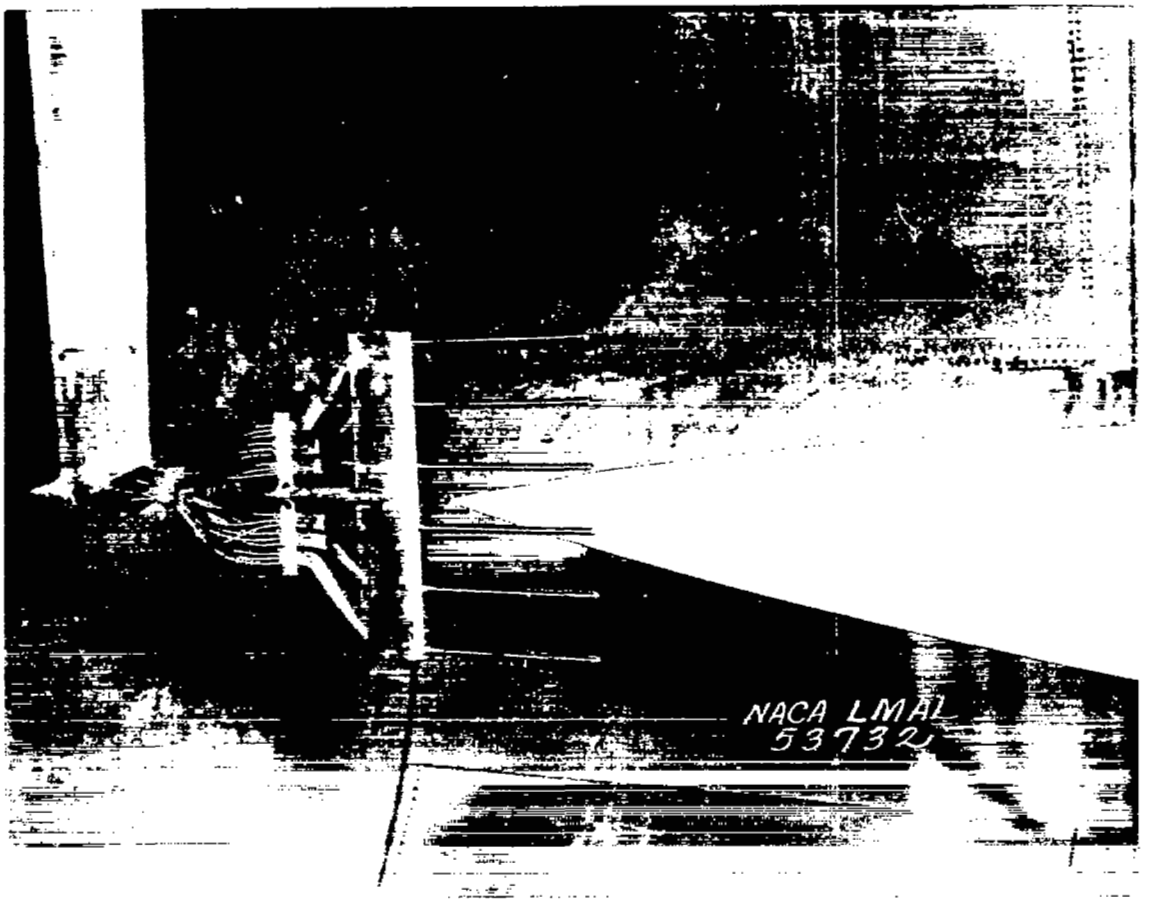

(a) Photograph of rake head.

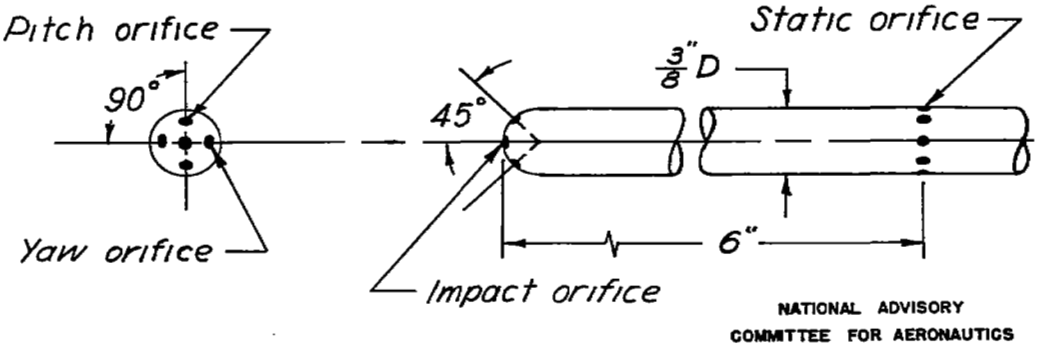

(b) Sketch of tube head.

Figure 5.- Langley 19-foot pressure tunnel air-stream survey rake.

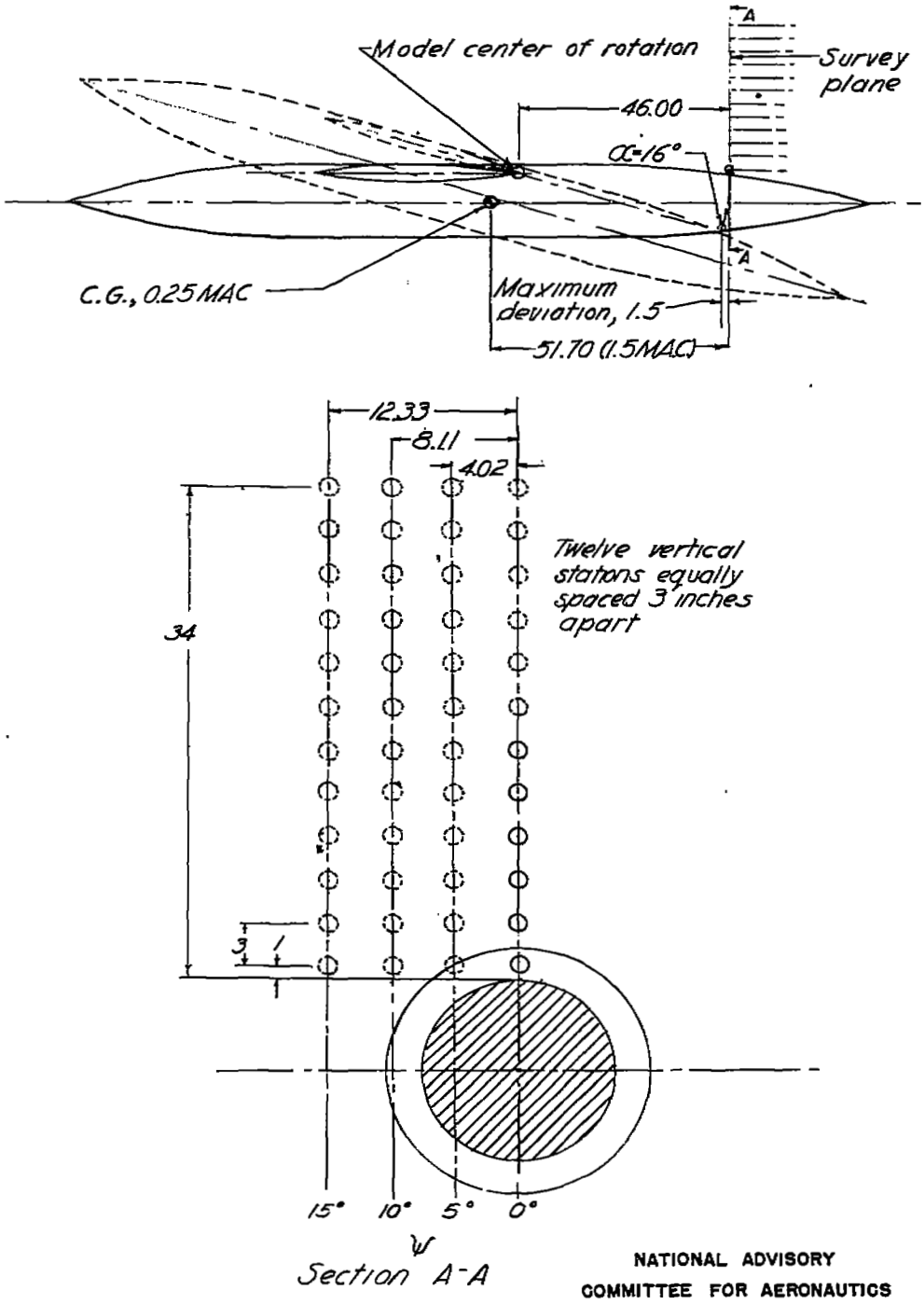

(c) Location of air-stream survey points.

Figure 5.— Concluded.

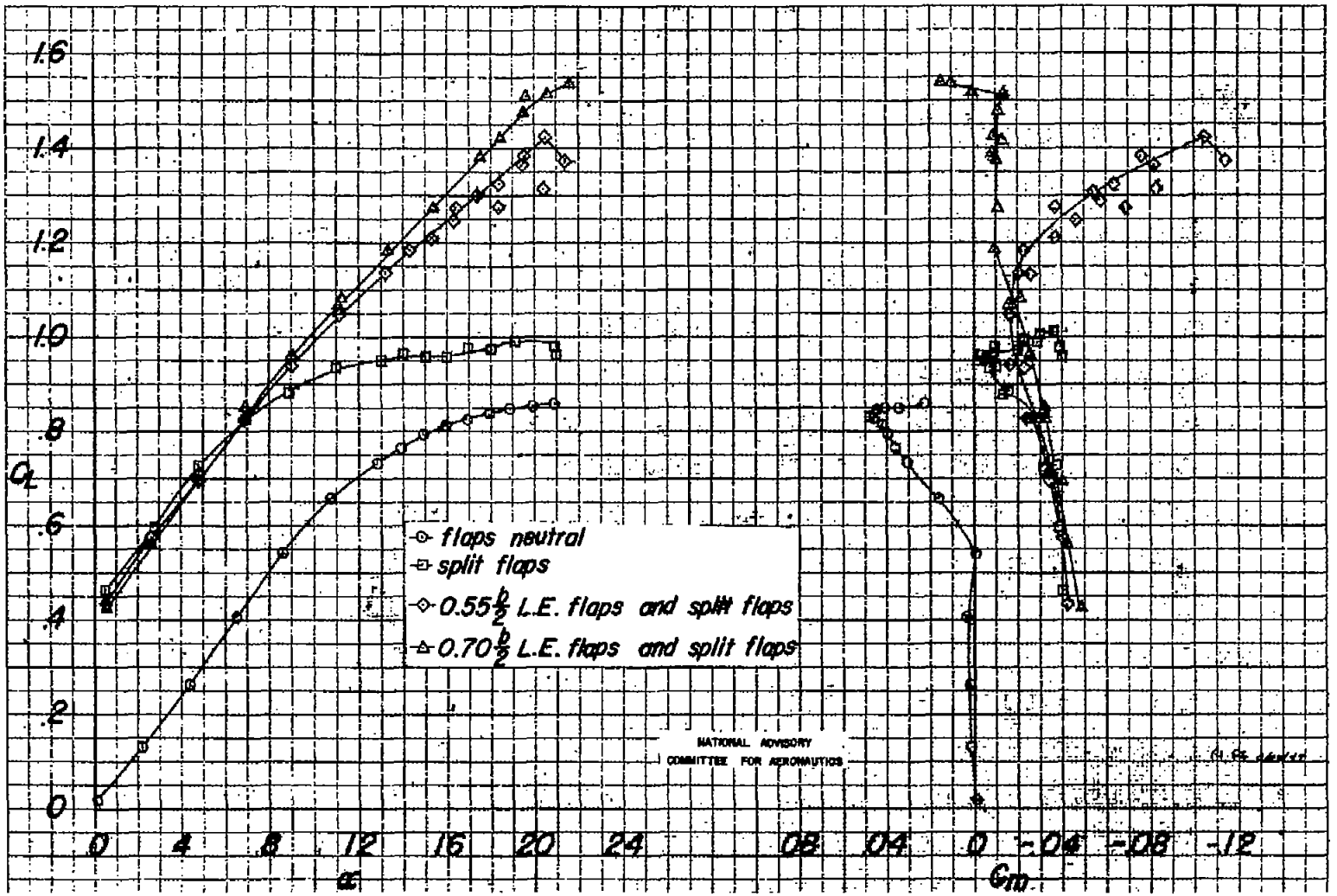

(a) α and C_m against C_L.

Figure 6.– Aerodynamic characteristics of a 42° sweptback wing of circular-arc airfoil sections. Plain wing; split flaps deflected; and 0.55 $\frac{b}{2}$ and 0.70 $\frac{b}{2}$ leading-edge flaps in conjunction with split flaps deflected.

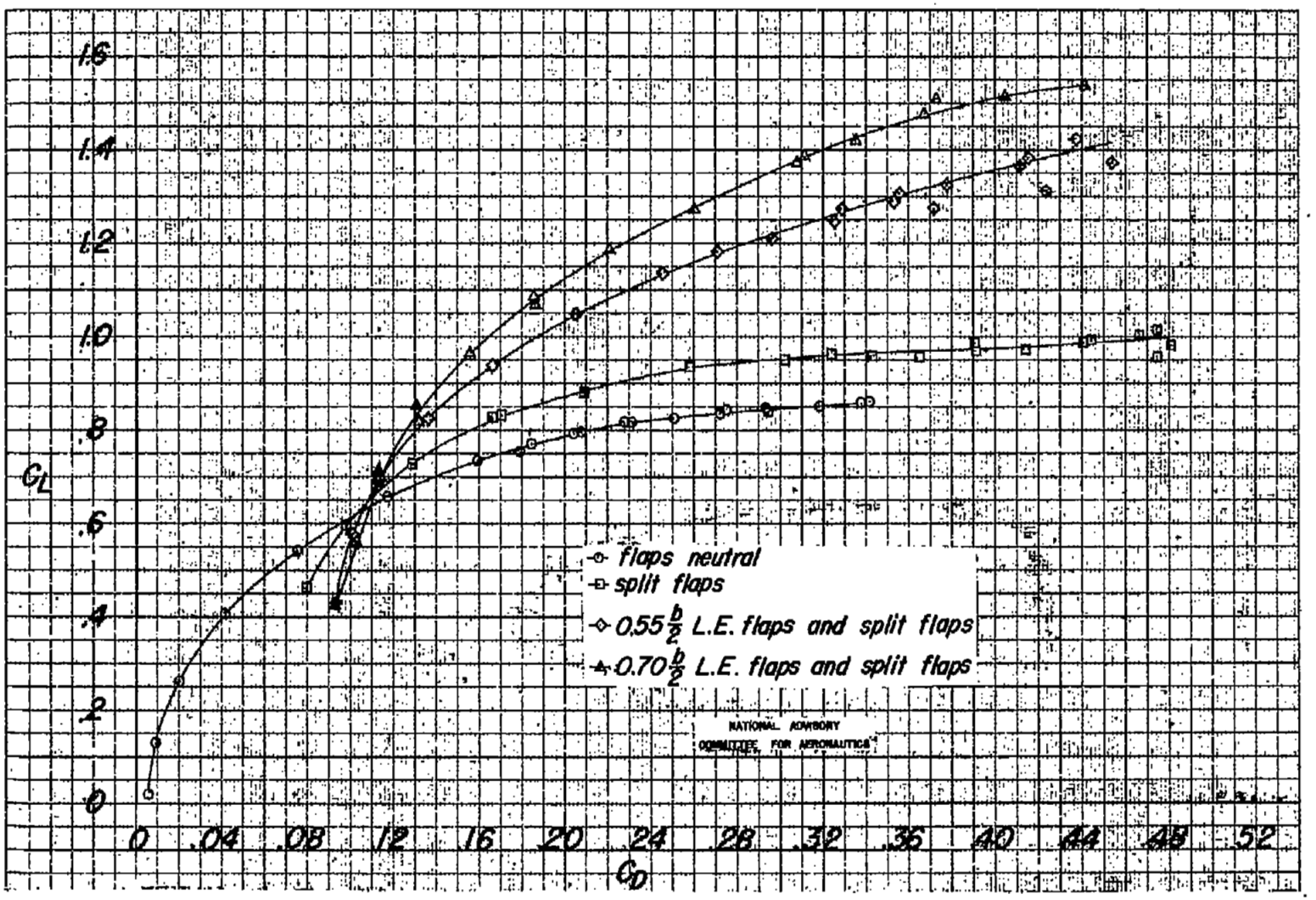

(b) C_D against C_L.

Figure 6.- Concluded.

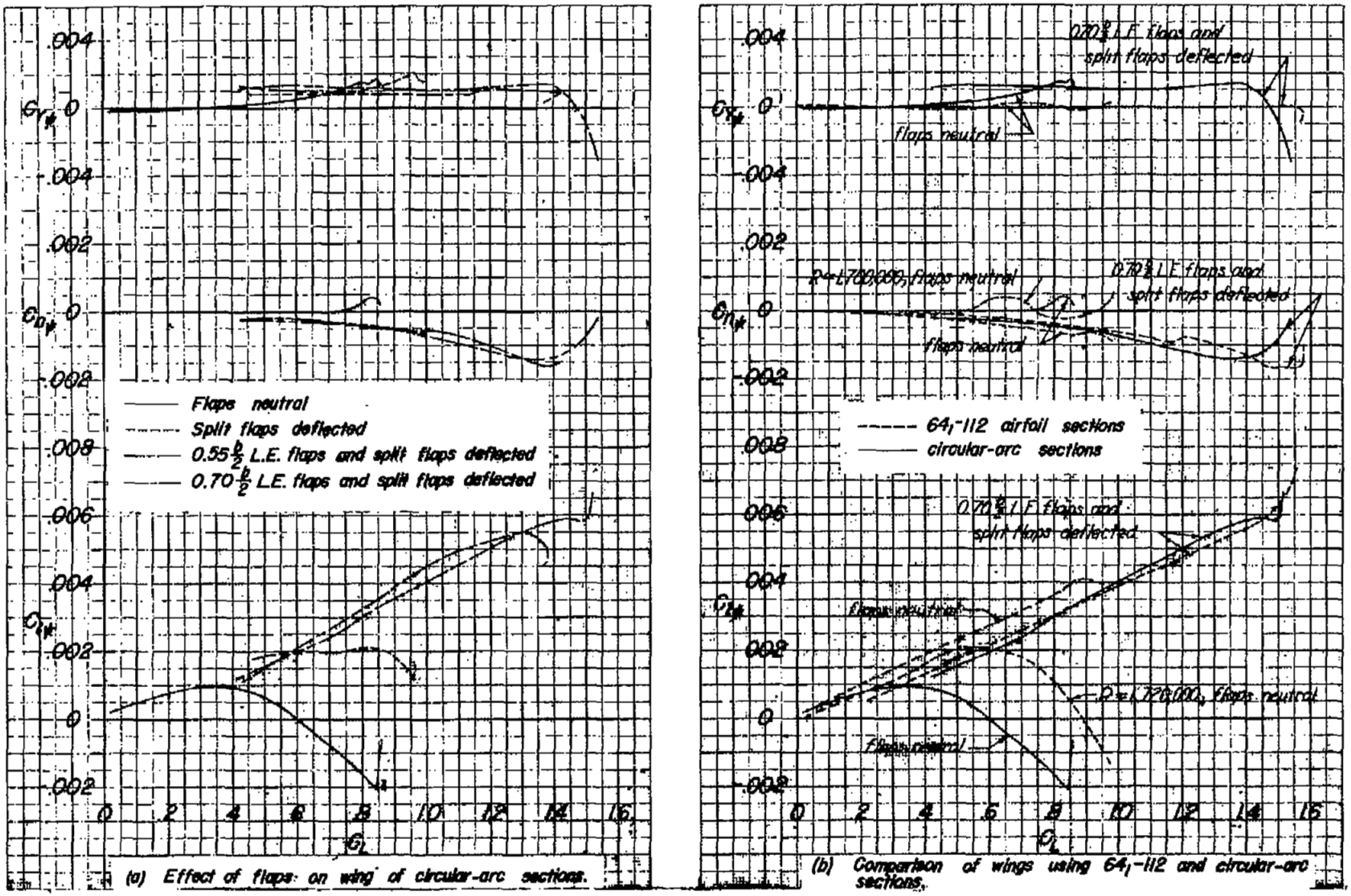

Figure 7 - Variation of C_{l_ψ}, C_{n_ψ}, and C_{Y_ψ} with lift coefficient for 42° sweptback wings of 64_1-112 and symmetrical circular-arc sections. $R \approx 5{,}300{,}000$ except as noted.

NATIONAL ADVISORY
COMMITTEE FOR AERONAUTICS

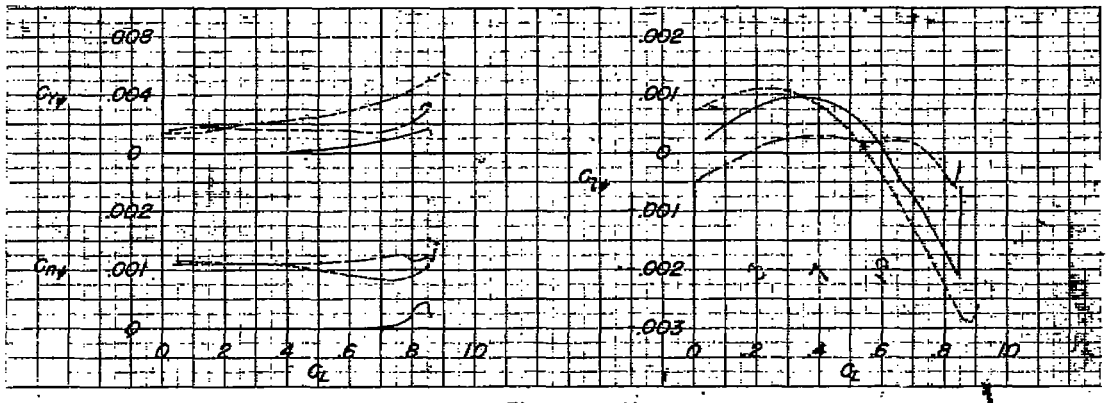

(a) Flaps neutral.

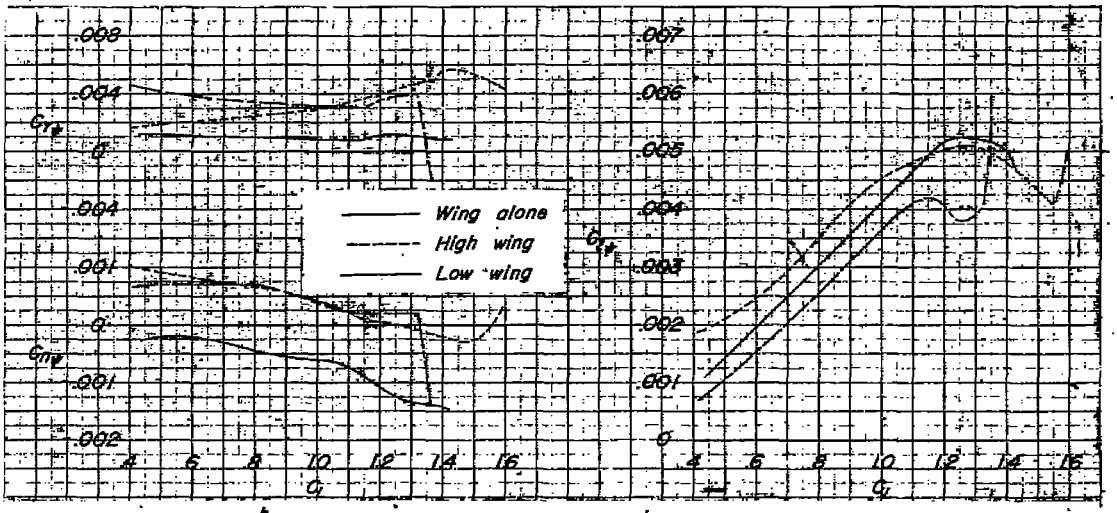

(b) 0.55 $\frac{b}{2}$ leading-edge flaps and 0.50 $\frac{b}{2}$ split flaps.

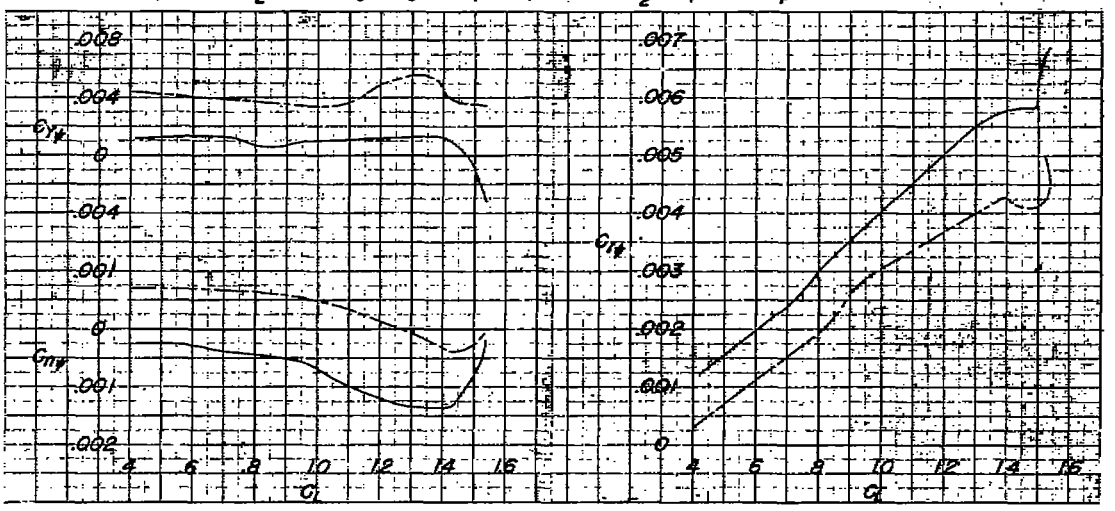

(c) 0.70 $\frac{b}{2}$ leading-edge flaps and 0.50 $\frac{b}{2}$ split flaps.

NATIONAL ADVISORY COMMITTEE FOR AERONAUTICS

Figure 8.— Variation of C_{l_ψ}, C_{n_ψ}, and C_{Y_ψ} with C_L of a 42° sweptback wing of symmetrical circular-arc sections, tested alone and with a fuselage, in high-wing and low-wing combinations.

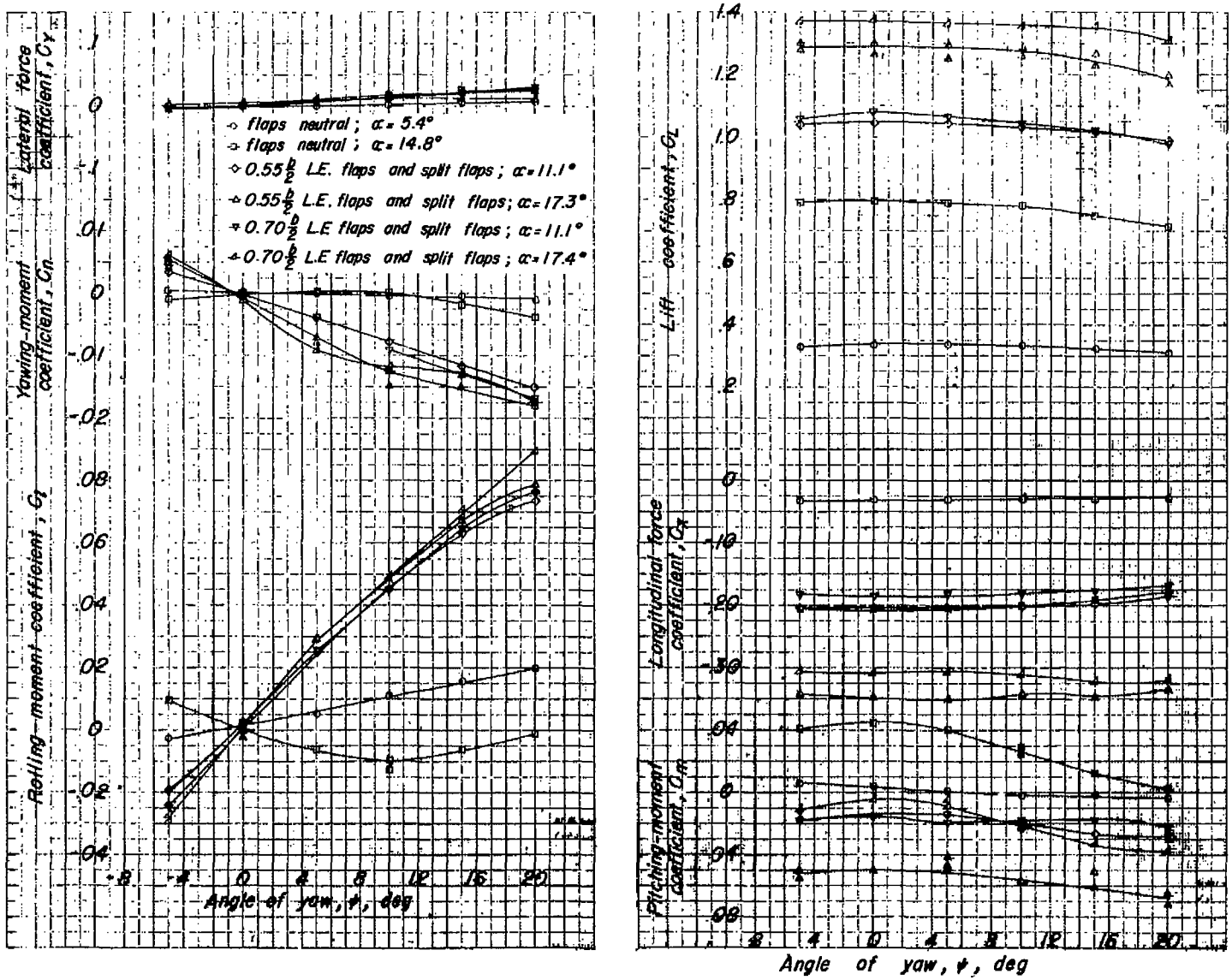

Figure 9.- Variation of aerodynamic characteristics with angle of yaw for a 42° sweptback wing of circular-arc sections. Flaps neutral; 0.55 $\frac{b}{2}$ and 0.70 $\frac{b}{2}$ leading-edge flaps and split flaps deflected.

NATIONAL ADVISORY
COMMITTEE FOR AERONAUTICS

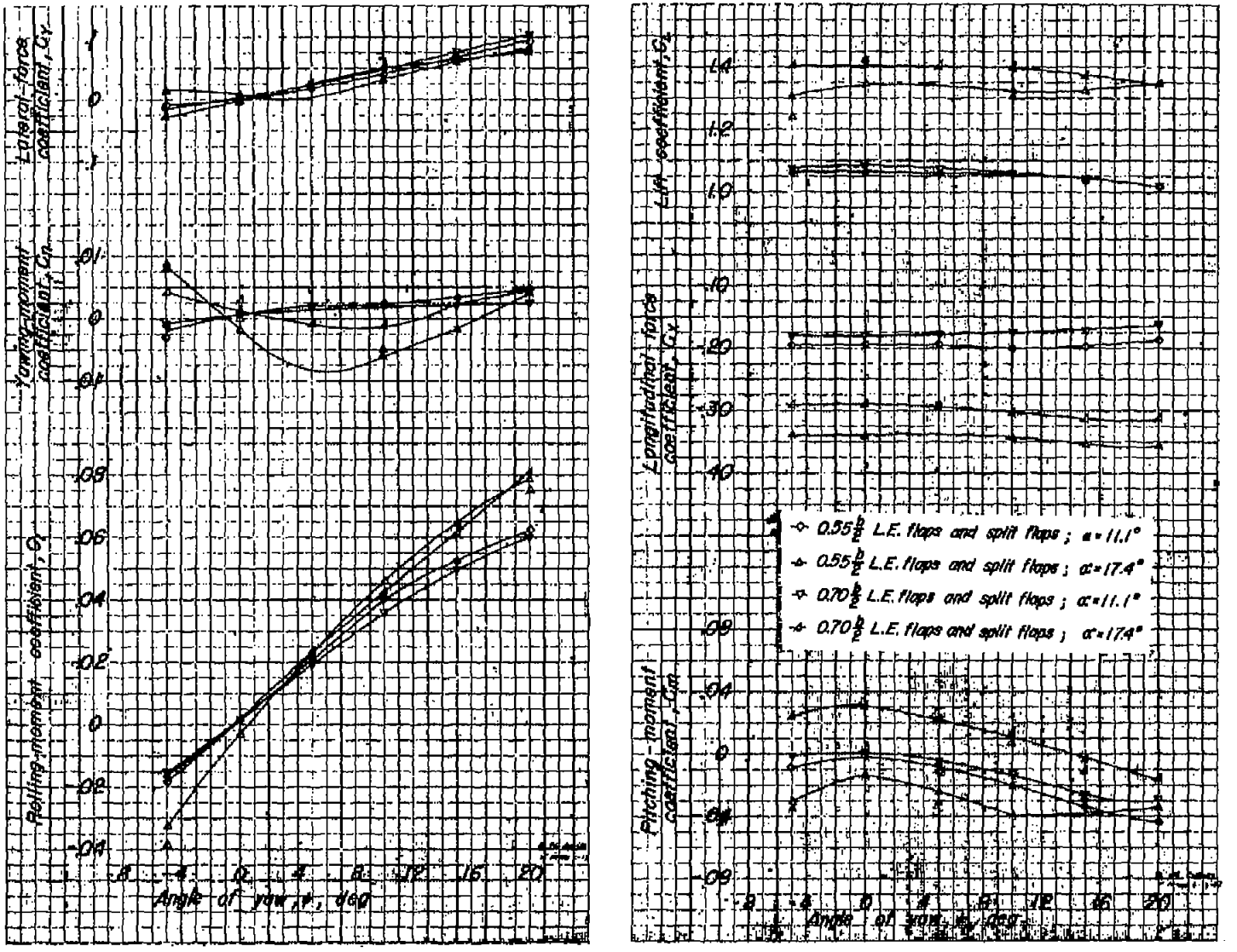

Figure 10.– Variation of aerodynamic characteristics with angle of yaw for a 42° sweptback wing of circular-arc sections. $0.55\frac{b}{2}$ and $0.70\frac{b}{2}$ leading-edge flaps in conjunction with split flaps. Low-wing combination.

NATIONAL ADVISORY
COMMITTEE FOR AERONAUTICS

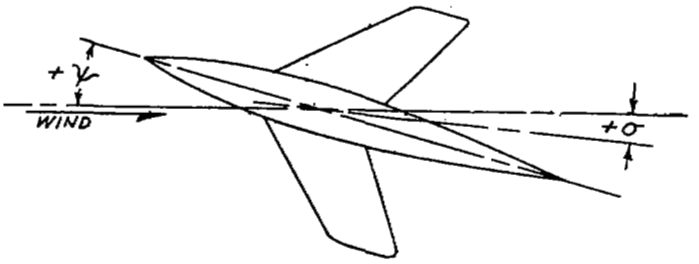

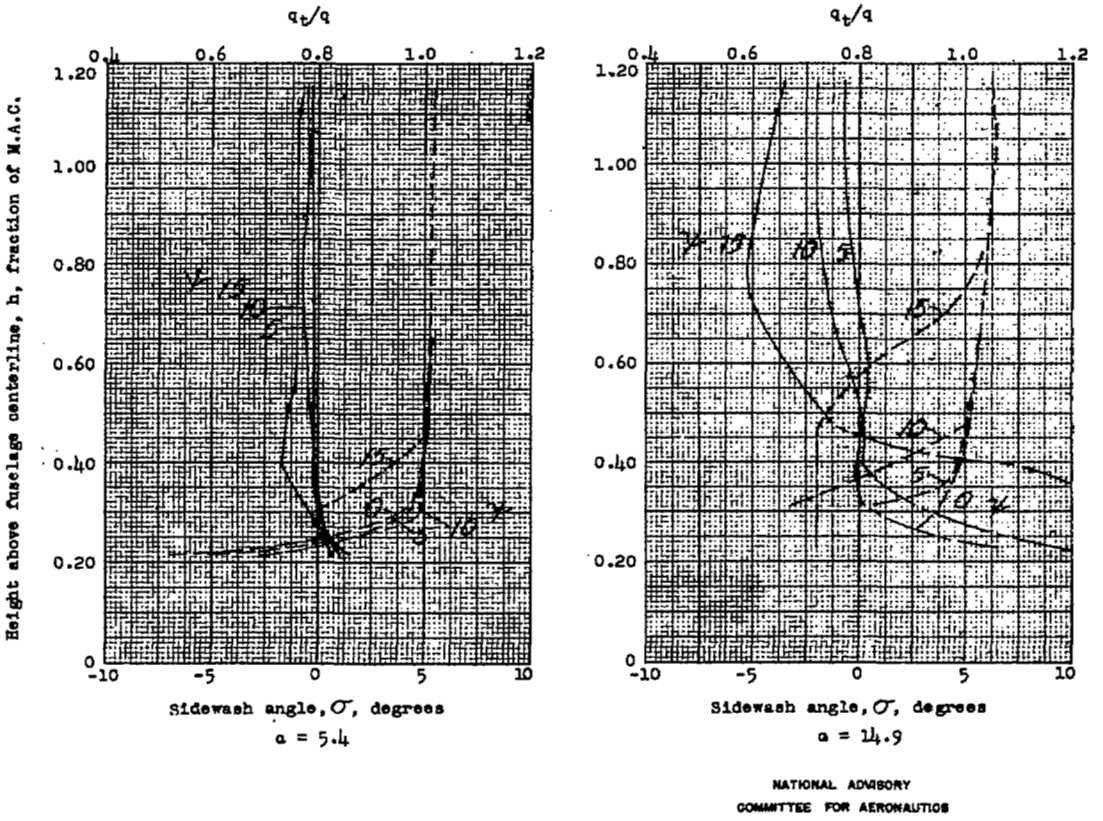

(a) High wing.

Figure 11.- Variation of sidewash angle and dynamic-pressure ratio with height above fuselage centerline. Flaps neutral. R = 5,300,000; M = 0.11.

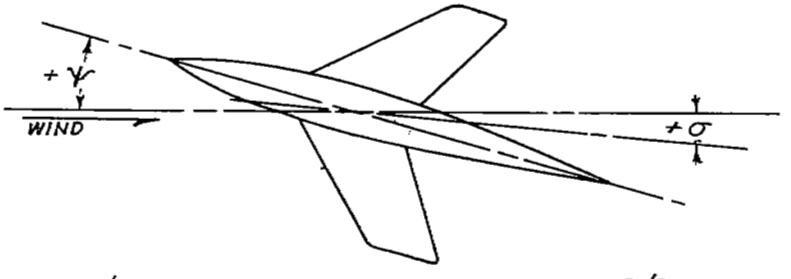

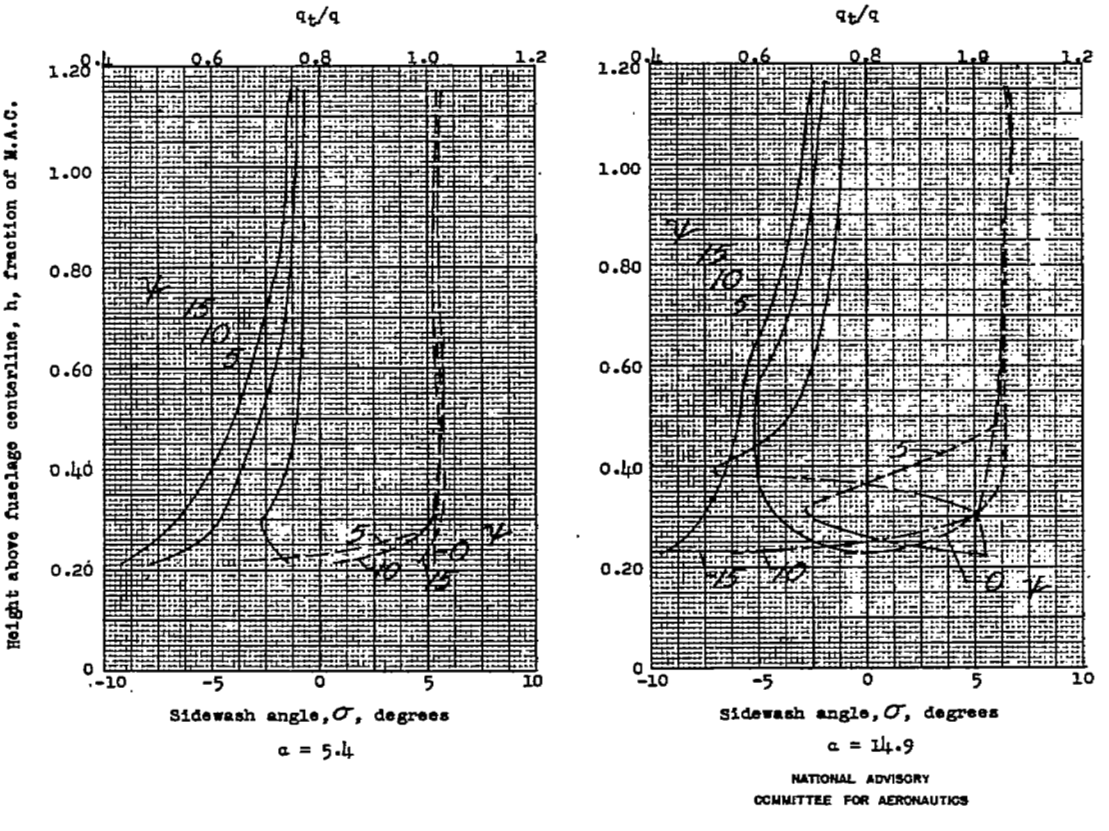

——————— σ

— — — — — — — — q_t/q

——— — ——— — ——— extrapolated values

(b) Low wing.

Figure 11.- Concluded.

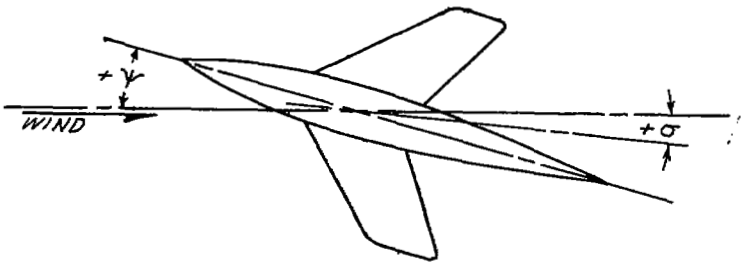

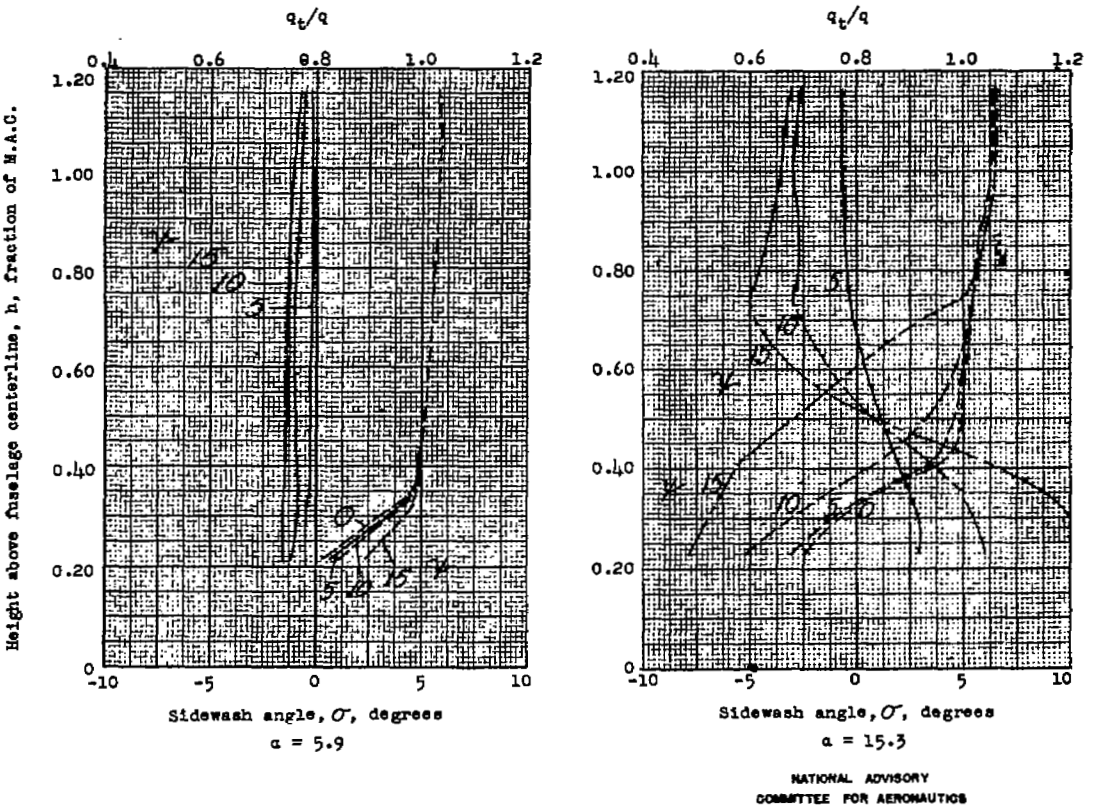

(a) Wing alone.

Figure 12.- Variation of sidewash angle and dynamic-pressure ratio with height above fuselage centerline. Centerline for wing alone same as for high wing. 0.55 b/2 leading-edge flaps and split flaps deflected; R = 5,300,000; M = 0.11.

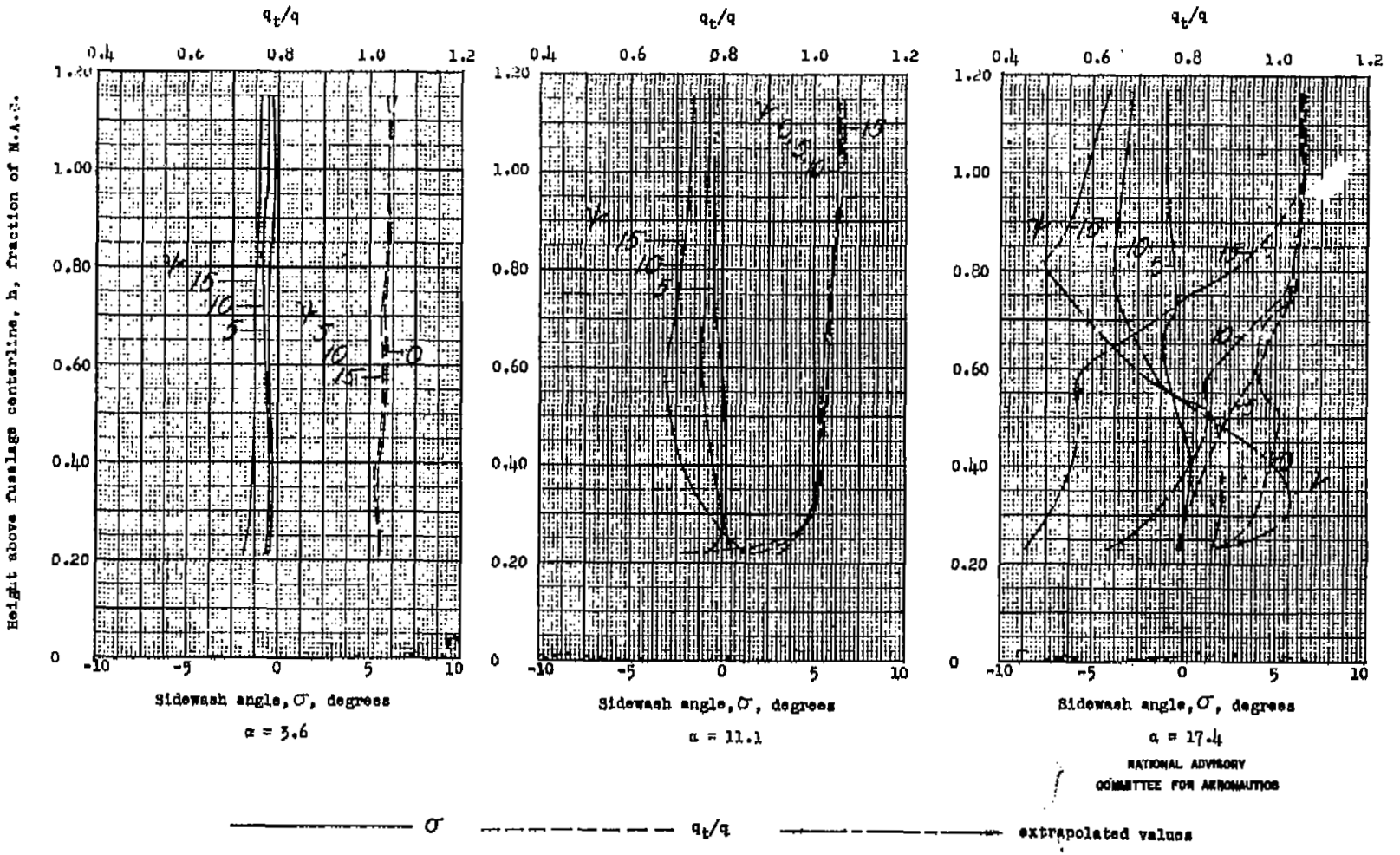

(b) High-wing combination.

Figure 12.- Continued.

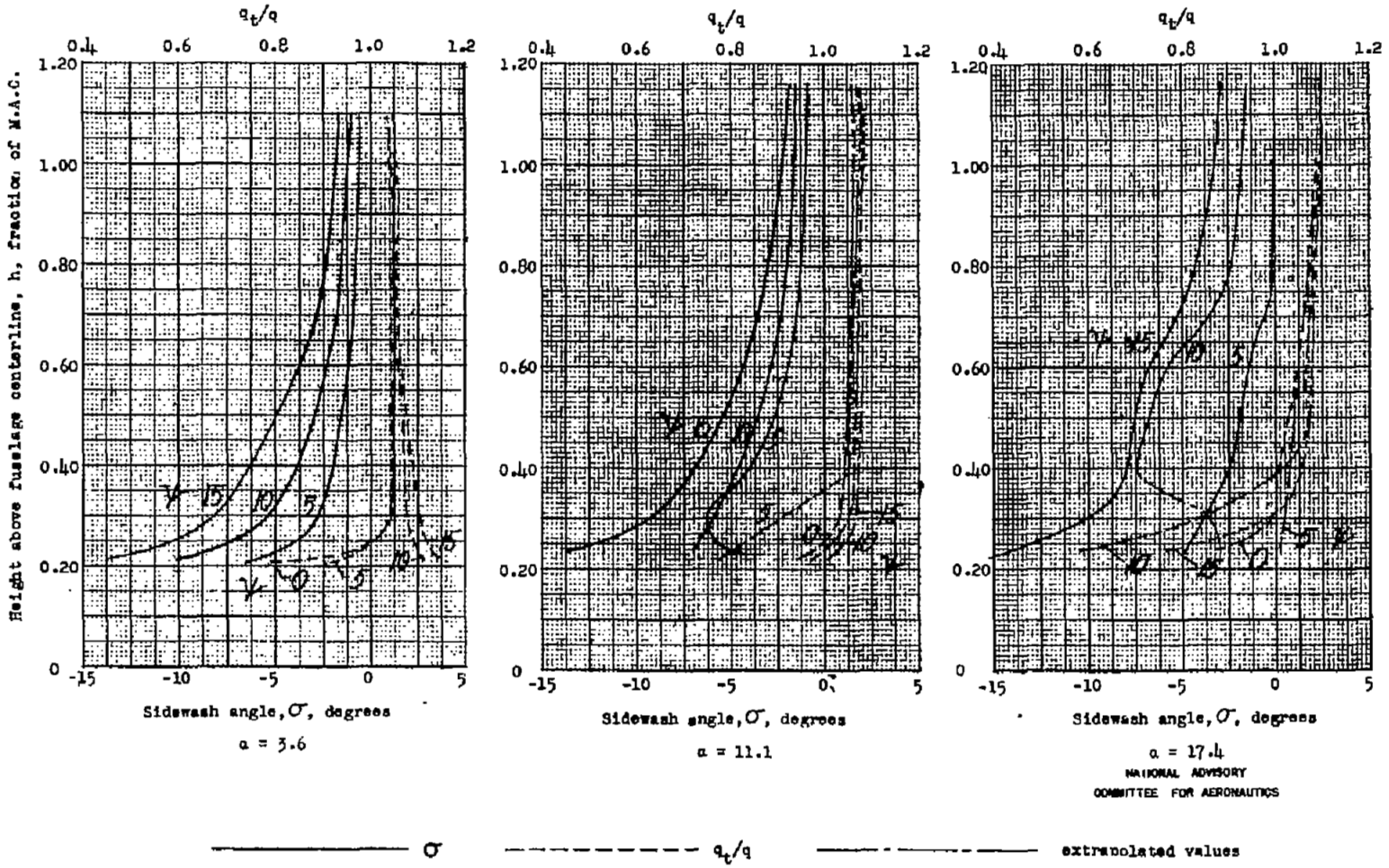

(c) Low-wing combination.

Figure 12.- Concluded.